Research

Ultrasonic pulse velocity and artificial neural network prediction of high-temperature damaged concrete splitting strength

Hatem Almasaeid[1]

Abstract

To examine the integrity of any structure following a fire, assessments of the impact of high temperatures on concrete are essential, particularly its decreased in tensile strength. Destructive examinations, such as the extraction of concrete cores, can pose significant cost and safety challenges, particularly when applied to structures that have already sustained damage. Consequently, for assessing damaged concrete, non-destructive in-situ tests are the favored approach. This study aims to develop an artificial neural network model utilizing data from ultrasonic pulse velocity measurements. The model's purpose is to assess the tensile splitting strength of concrete subjected to elevated temperatures, ranging from 200 to 800 °C. The splitting strength investigation showed that increasing the exposure temperature from 200 to 800°C results in splitting strength reduction of 15 to 75% respectively. Also, the ultrasonic pulse velocity experienced a reduction of 85% when the exposure temperature reaches 800 °C. In addition, the results of the artificial neural network model indicated that ultrasonic pulse velocity and temperature data were sufficient to reasonably forecast the tensile splitting strength of concrete. The developed artificial neural network model has a coefficient of determination (R^2) of 0.943, a mean absolute relative error (MARE) of 5.028, and an average squared error (ASE) of 0.000907.

Article Highlights

- ANN modelling could predict concrete strength after fire exposure accurately.
- Concrete splitting strength decreases significantly at higher temperatures (75% at 800 °C).
- Non-destructive testing offers safe and accurate assessments for fire damaged concrete.

1 Introduction

Although concrete is a well-known long-lasting building material, over the course of its life, it might be subjected to a number of unintentional or environmental events that lead to its deterioration. Therefore, it is crucial to evaluate and restore prevailing concrete structures. The occurrence of high temperatures or fire close to concrete structural components, particularly in high-rises, tunnels, and drilling platform constructions, is one of the most hazardous

✉ Hatem Almasaeid, almasaeid.h@aabu.edu.jo | ¹Civil Engineering Department, Faculty of Engineering, Al Al-Bayt University, Mafraq 25113, Jordan.

scenarios. Fires may cause temperatures to soar to 1100 °C in structures and even up to 1350 °C in tunnels, thereby, severely ravaging concrete buildings. Under certain circumstances, even much lower temperatures can dangerously alter the chemical, physical, and mechanical characteristics of concrete, thereby, jeopardising the strength of the concrete [1, 2]. The variations in concrete as a function of temperature depend on a variety of factors, including the constitution of the concrete, the ratio of water to cement, and the kind of aggregate utilised to name a few. The heating rate and the length of time that the concrete is exposed to high temperatures are also significant considerations [3]. This is because a rise in temperature causes the evaporation of water, the dehydration of calcium silicate hydrates (C–S–H) gel, the decomposition of calcium hydroxide (Ca(OH)$_2$) and calcium aluminate (CaAl$_2$O$_4$), and changes in the aggregate. As a result of these modifications, the strength and elasticity modulus of concrete steadily diminish and the strength loss accelerates at temperatures exceeding 300 °C. Concrete typically loses 50 to 60% of its compressive strength (CS) once the 500 °C mark is reached, at which point it is deemed entirely damaged [4–8].

Unlike other building materials, concrete has good fire-resistant qualities. However, because of fire-induced spalling, its strength rapidly degrades at high temperatures, which can weaken or even destroy multiple layers of concrete and leave the steel reinforcements within them exposed to a hot environment [9, 10]. The spalling failures observed in concrete exhibit a range of characteristics, spanning from gradual (the ongoing detachment of small scales from the specimen's surface when exposed to radiant heating) to abrupt and forceful (the sudden disintegration of the specimen, accompanied by the release of a significant amount of energy that propels shattered concrete fragments in various directions at high speeds). It has been hypothesized that the heightened vulnerability concrete to sudden, explosive spalling at elevated temperatures is, in part, attributable to low permeability or high hearing rate. This decreased permeability or rapid heating rate restricts the escape of water vapor from the concrete's pores, resulting in the accumulation of pressure within these voids [11, 12]. As the temperature increases, so does this vapor pressure, escalating until internal stresses reach a critical point, ultimately leading to an abrupt, explosive spalling event. Thus, spalling occurs when water vapour causes the pore pressure within layers of heated concrete to surpass the tensile strength (TS) of the concrete [13–15].

In concrete, TS is significantly lower than its CS. This is evidenced by the ease with which cracks can spread under tensile loads compared to compressive stresses, under which cracks exhibit a tendency to close. As such, the TS of concrete is frequently overlooked when calculating its strength at room temperature. TS, however, may be much more significant in fire-related situations when a component of the concrete experiences fire-induced spalling [16–18].

The detection of possible high-temperature damage to structures and the identification of deterioration levels can both benefit greatly from in-situ evaluation and scrutiny. Due to their relative speed, lower cost, ease of use, and ability to minimise structural damage, non-destructive tests (NDTs) are favoured over destructive tests (DTs) [19–23]. As a few of the physical qualities of concrete can be associated with the strength of concrete, various NDTs have been formulated. Ultrasonic pulse velocity (UPV) and rebound number (RN) techniques are of the most used NDTs used in the assessing concrete properties [24]. The utilization of NDTs for high-temperature damaged concrete were investigation by several researchers [25]. Thermally damaged concrete assessment based on UPV results was studied by Colombo and Felicetti. The results of their study illustrated that UPV is correlated to the concrete mechanical properties. Also, UPV was found to be sensitive to thermal damage [26]. In addition, Abed and Brito studied the evaluation of compressive strength, residual density, flexural strength and UPV of high-performance self-compacting concrete after exposure to elevated temperatures. The results of their study indicated that the reduction in UPV results after exposure is highly correlated to concrete properties [27]. Furthermore, effects of high temperatures up to 800 °C on UPV results in concrete have been studied by Chung. And it was found that pulse velocity decreased with increase of the exposure temperature [28]. However, NDTs cannot measure the concrete strength directly. In fact, NDTs outputs such as UPV are mainly physical parameters. Nevertheless, in several cases, the theoretical relationships between NDT results and concrete strength are unknown. So that, empirical relations are usually developed in order to describe these relations. One of the popular methods to draw the relation between NDTs and concrete strength is artificial neural networks [29, 30].

Artificial neural networks (ANNs); which are algorithms that mimic human neurons; is one of the many cutting-edge machine learning prediction techniques used in recent decades. These neurons are displayed as biological neuron models as well as conceptual constituents for circuits that can execute computational actions. An ANN processes information by utilizing a connectionist technique for calculations and is made up of interconnected clusters of artificial neurons. As they also use a non-linear activation function, ANNs can also elucidate and distinguish subtle non-linear correlations between a large number of variables in exceedingly intricate datasets. By stowing the data in the connection weights, it may also relate and correlate various factors to one another, thereby, avoiding the challenges of absent theoretical foundations [31–33]. If properly trained, ANNs will be able to predict concrete properties will acceptable accuracy compared to linear or non-linear regression [34].

In previously published researchs, ANN modelling was employed in predicting the concrete mechanical characteristics based on NDTs results and proved its ability to model these characteristics with minimal error values [35, 36]. In his study, Demir used the UPV and rebound number to develop an ANN to forecast the CS of a concrete. The proposed ANN model was able to highly accurately associate concrete strength with the results of the NDTs, with a coefficient of determination (R^2) of 0.975 [37]. Also, Atici used ANN and regression modelling in predicting the strength of mineral admixture concrete based on UPV and RN testing results. The modelling results showed that combining the NDTs results using ANN to predict the concrete properties is applicable with acceptable accuracy [38]. In addition, ANN was utilized by the researchers in predicting the Splitting Tensile Strength (SS) of concrete [39]. Ray et al. investigated the ability to predict concrete CS and SS using ANN and response surface methodology. The study showed that ANN is able to predict the concrete strength with acceptable accuracy based on concrete ingredients [40]. In addition, Behnood et al. used ANN, model tree and support vector machine in evaluating the concrete SS based on CS. The results illustrated that ANN along with other methods can predict the SS of concretes made with and without steel fiber reinforcement with satisfactory accuracy [41]. In the other hand, machine-learning methods such as ANN, proved their ability to be used in assessing the concrete strength under various conditions such as thermally-damaged concrete [42–44]. Candelaria et al. studied the possibility of using UPV in assessing early fire damage in concrete. The study analyzed the applicability of utilizing both linear and nonlinear parameters from UPV test and the applicability of machine learning in assessing the thermal damage of concrete samples. The results illustrated that there is a high correlation between the pulse velocity and the concrete strength [45]. In the other hand, Trtink et al. studied the relations between UPV, static and dynamic Young's modulus and shear modulus. In their study, the influence of initial concrete temperature, aggregate, type of cement, environmental temperature, and water to cement ratio was determined by experimental testing and correlated to concrete properties using ANN modeling. The results showed that ANN could successfully utilized in modelling the pulse velocity–strength relationship [24]. Furthermore, Almasaeid et al. studied the possibility of predicting the concrete thermal-damage levels by combining NDTs results using ANN modelling. The study included UPV and RN testing. The results of the study indicated that ANN is able to anticipate the thermal damage level in concrete CS using only NDTs results with acceptable accuracy [6]. So that, based on the previous studies, it is concluded that ANN is able to predict the mechanical properties of thermally-damaged concrete based on NDT results only. However, none of the published researches utilized ANN and NDT to anticipate the SS of thermally-damaged concrete.

As previous research did not employ an ANN-based model for predicting concrete splitting strength (SS) based on non-destructive testing (NDT) results, this current study focuses on the development of an ANN model. The model is built using data obtained from casting multiple concrete samples with varying mixture ratios and exposing them to high temperatures ranging from 200 to 800°C to induce damage. Subsequently, these samples underwent both destructive testing (DT), specifically a splitting strength (SS) test, and non-destructive testing (NDT), namely an ultrasonic pulse velocity (UPV) test.

The objective of this study is to forecast the SS of both the damaged and undamaged concrete samples by utilizing the experimental test results through the ANN model. The development of such a model holds the potential to enable practitioners in the field to assess concrete condition without resorting to destructive tests, thereby reducing costs and enhancing safety when dealing with fire-damaged concrete structures.

2 Materials and methods

2.1 Introduction

In this research, six concrete mixtures were prepared using ordinary Portland cement with the aim of subjecting them to various elevated temperatures to induce damage. Subsequently, both destructive and non-destructive tests were conducted to assess their splitting tensile strength. The following subsections describes the utilized materials, damage process, and tests performed in this study.

2.2 Concrete mixes

Portland cement was used to prepare multiple samples containing various types and quantities of concrete mixtures to cover a wide variety of SSs. Tables 1 and 2 tabulates the cement properties and characteristics of the aggregates used respectively.

Six primary samples, each with different proportions of concrete and aggregates, were prepared (Table 3). The samples were poured into 150×300 mm cylinders and allowed to cure for seven and 21 days in water and air, respectively. Twenty sub-samples were created for each of the six primary samples and split into five groups of four before they were subjected to five different levels of high temperatures.

2.3 Temperature damage

An electric furnace was used to heat the concrete sub-samples to high temperatures and damage them. Over a 2-h period, the concrete sub-samples were heated to temperature ranges of 200 to 800 °C. The heating schedule and the electric furnace ensured that the desired temperatures were reached by a heating rate of 3 °C/min maintained at the desired temperature for 120 min before the sub-samples were gradually cooled in the furnace for 24 h before exposure them to laboratory environment.

Table 1 Cement chemical and physical properties

Oxide	Content (%)	Property	Value
SiO_2	20.72	Specific gravity	3.15
$AleO_3$	5.58	Fineness	325 m^2/kg
Fe_2O_3	3.31	Initial setting time	115 min
CaO	61.74	Final setting time	225 min
MgO	2.47		
Na_2O	0.17		
K_2O	0.79		
Loss of ignitions	2.12		

Table 2 Physical properties of the aggregate

	Coarse aggregate	Fine aggregate
Maximum aggregate size (mm)	12.5	4.75
Bulk specific gravity	2.66	2.62
Absorption (%)	1.18	1.22
Fineness modulus	–	2.78

Table 3 Proportions of the concrete mixtures

Mix	W/C	Content in kg/m³				Average CS (MPa)	Average SS (MPa)
		Cement	Coarse aggregate	Fine aggregate	Water		
1	0.53	290	968	694	153	16.8	3.16
2	0.50	310	968	694	155	25.2	3.63
3	0.47	340	985	646	160	28.6	3.50
4	0.44	370	1008	605	163	36.1	3.88
5	0.41	390	1008	600	160	39.4	3.98
6	0.38	415	1023	583	157	46.4	4.18

2.4 Sample testing

The UPV test was used as the NDT and the SS test was used as the DT to examine and determine the SS of the samples.

2.4.1 Ultrasonic pulse velocity test

A generator and a receiver transistor are typically used to gauge the UPV travelling through the concrete. These tests can be conducted either in-situ or in a lab. The American Society for Testing and Materials (ASTM) C597 document outlines the test [46]. Three alternative configurations; direct (D), semi-direct (S), and indirect (I), can be used to conduct a UPV test. This present study only used the direct UPV test setting. In this research, Matest C396N UPV tester is utilized with a range of 0–3000 μs, accuracy of 0.1 μs, and 55 Hz probs.

2.4.2 Splitting tensile strength test

The cylinder-splitting test was used to measure the TS of the concrete. To obtain the experimental SS of the concrete, a compression-testing machine (CTM) was used to examine the 150 × 300 mm cylindrical samples. In addition to mixing propositions, Table 3 lists the average CS and SS results of the concrete mixes tested in this research.

3 Findings and analysis

Based on the data presented in Table 4 for UPV and SS testing outcomes, respectively, we observe a correlation similar to prior research [47]. This correlation affirms that UPV and SS exhibit a positive relationship. This connection between UPV and concrete strength can be attributed to the phenomenon where an increase in pulse velocity corresponds to a reduction in concrete void content, thereby enhancing concrete quality and strength [48]. A graphical representation of the correlation between UPV and SS for the intact samples is illustrated in Fig. 1.

Figure 2 provides an illustration of the impact of high temperatures on the SS of concrete. Figure 2a demonstrates that the SS decreases as the temperature rises. This decrease can be stated as:

$$\text{Reduction in SS(R\%)} = 100 - 100 * \frac{\text{damaged sample strength}}{\text{undamaged sample strength}} \tag{1}$$

Figure 2b shows the decrease in SS at various stages of exposure to high temperature based on Eq. 1. The SS of various sub-samples decreased by 15% as the temperature approached 200 °C. However, the decrease in SS increased to 35% when the temperature increased to 400 °C. The decrease in SS increased to 55% when the temperature was raised to 600 °C. Additionally, as the temperature rose to 800 °C, the decrease in SS approached 75% in some cases. Therefore, the residual SS of the damaged sub-sample was only 25% of its SS when it was undamaged.

Similarly, elevated temperatures had a significant impact on the UPV of the specimens. This effect is evident in Fig. 3, where a semi-linear relationship illustrates the decline in UPV as the temperature ascends from 200 to 800 °C. The decrease in pulse velocity is directly associated with a decrease in concrete quality and an increase in the occurrence of cracks. In addition, Fig. 4 illustrates the relation between the UPV and SS of high temperature damaged concrete.

4 Artificial neural network

4.1 Model structure and data

The ANN model of this present study was developed using the feed-forward error back-propagation (FB) technique. Layered structures are common in feed-forward error back-propagation (FB) networks. Every layer contains a predetermined number of units, comprising of inputs from the preceding layer, that are transmitted as outputs to the units of the subsequent layer. The input layer comprises input units, which are thought to impact the outputs, while the

Table 4 Results of experimental tests

Mix	Sample	No Damage		Damage at 200 °C		Damage at 400 °C		Damage at 600 °C		Damage at 800 °C	
		UPV (m/sec)	Splitting Strength (MPa)	UPV (m/sec)	Splitting Strength (MPa)	UPV (m/sec)	Splitting Strength (MPa)	UPV (m/sec)	Splitting Strength (MPa)	UPV (m/sec)	Splitting Strength (MPa)
1	1–1	3886	3.08	3025	2.70	1974	2.14	1116	1.38	505	0.87
	1–2	3935	3.37	3058	2.91	2106	2.26	1207	1.58	945	0.97
	1–3	3708	3.01	2859	2.51	2107	2.02	1197	1.30	660	0.83
	1–4	4193	3.19	3273	2.69	2068	2.07	1171	1.46	634	0.95
	Avg	3930	3.16	3054	2.70	2064	2.12	1173	1.43	686	0.90
2	2–1	3963	3.44	3090	3.02	2232	2.39	1323	1.54	992	1.14
	2–2	4271	3.58	3343	3.21	2351	2.46	1403	1.66	1065	1.09
	2–3	4455	3.40	3493	2.86	2403	2.16	1435	1.35	1090	0.90
	2–4	4258	3.57	3328	3.13	2359	2.21	1404	1.59	1060	1.04
	Avg	4236	3.50	3314	3.05	2337	2.30	1391	1.54	1051	1.04
3	3–1	3988	3.57	3112	3.09	2171	2.48	1274	1.59	1094	1.09
	3–2	4335	3.77	3398	3.35	2193	2.55	1276	1.62	926	1.06
	3–3	4312	3.47	3373	2.85	2474	2.15	1491	1.48	1033	1.04
	3–4	4020	3.69	3126	3.23	2320	2.36	1372	1.65	908	1.12
	Avg	4164	3.62	3252	3.13	2289	2.38	1353	1.59	990	1.08
4	4–1	4254	3.78	3338	3.38	2185	2.66	1285	1.63	839	1.10
	4–2	4200	4.18	3283	3.58	2339	2.74	1393	1.86	938	1.19
	4–3	4611	3.55	3626	3.18	2531	2.37	1537	1.56	1083	0.96
	4–4	4414	3.99	3462	3.44	2473	2.47	1494	1.73	1041	1.08
	Avg	4370	3.87	3427	3.39	2382	2.56	1427	1.69	976	1.08
5	5–1	4213	3.92	3303	3.41	2214	2.85	1309	1.70	864	1.12
	5–2	4405	4.28	3458	3.73	2303	2.81	1364	1.86	790	1.26
	5–3	4574	3.68	3595	3.26	2496	2.45	1509	1.63	934	0.97
	5–4	4508	4.04	3541	3.39	2396	2.53	1433	1.79	856	1.16
	Avg	4425	3.98	3474	3.44	2352	2.66	1404	1.75	861	1.13
6	6–1	4420	4.01	3479	3.36	2413	2.87	1468	1.86	1402	1.22
	6–2	4607	4.53	3629	3.86	2452	2.95	1484	1.87	1294	1.38
	6–3	4703	3.92	3705	3.33	2423	2.42	1607	1.77	1080	1.15
	6–4	4712	4.25	3715	3.71	2613	2.66	1606	1.94	1182	1.26
	Avg	4611	4.18	3632	3.56	2475	2.72	1541	1.86	1240	1.25

Fig. 1 Correlation between splitting strength of undamaged concrete and **a** UPV testing results **b** compressive strength

(a)

(b)
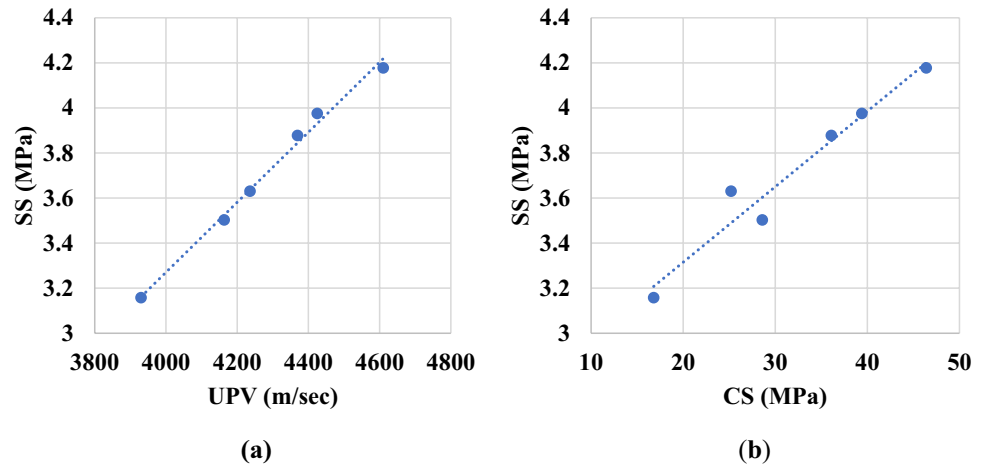
Fig. 2 Effect of high-temperature level on: **a** concrete splitting strength **b** Reduction of SS in concrete

(a)

(b)
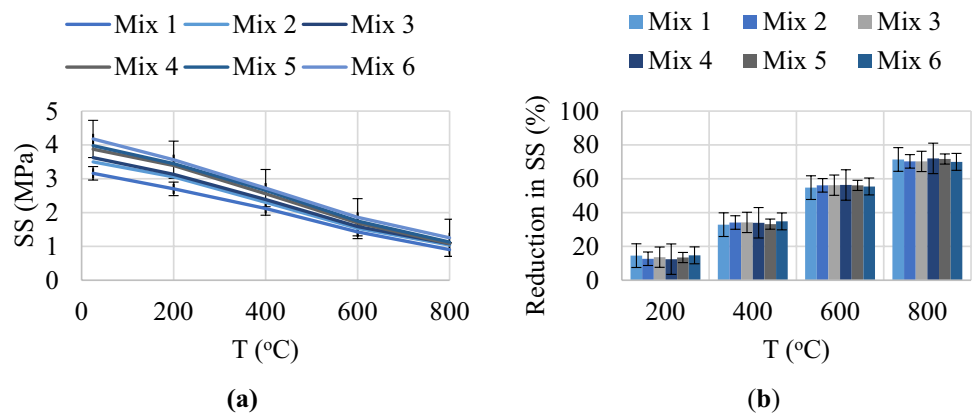
Fig. 3 Effect of exposure temperature level on the UPV results
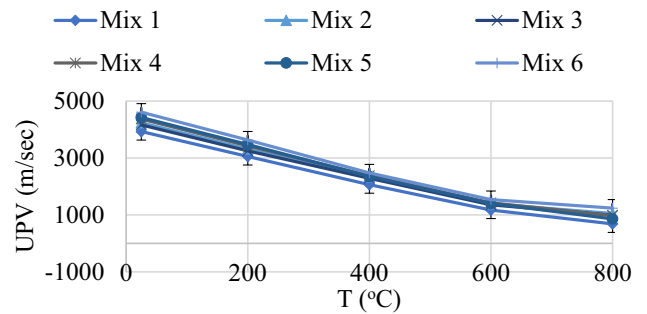
Fig. 4 Effect of high temperatures on the relation between concrete SS and UPV
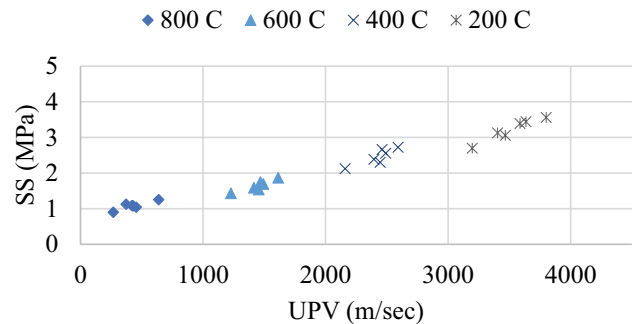
output layer comprises outputs units. Several hidden layers between these two layers contain hidden nodes units, which allow data to flow from the input to the output and vice versa through interconnected links [49, 50]. Most FB ANN applications have adopted network designs with just one hidden layer [51]. An FB network must go through three steps of training: feed-forward of the input training pattern, calculation and back-propagation of the related error, and adjustments to the weights of the interconnecting links. Following training, only the feed-forward stage computations are used in the network's application [52–54].

An ANN model was developed using 120 testing result datasets to forecast the SS of concrete. The datasets utilised in the modelling are listed in Table 4. The model was designed to have a sigmoidal function on one hidden layer.

If all inputs and outputs are normalised and scaled so that the entire data ranges from 0.1 to 0.9 prior to modelling, an ANN training can yield effective outcomes. The output of the ANN model must be denormalised because if the inputs are scaled, the output too will be scaled [55]. The parameters, their maximum and minimum values, standard deviations, and means for each parameter are listed in Table 5. The model was created to forecast SS based on the temperature and UPV values. Table 6 lists the parameters utilized in the developed model.

The training datasets were used to optimise the connections weights of the network's for various networks, with 1 to 10 hidden nodes, in the developed ANN model. The average squared errors (ASE), coefficient of determination (R^2), and mean absolute relative error (MARE) were computed and listed for every trained network. The trained networks were tested using the testing datasets that had not been employed to train the network. The network with the optimal number of hidden nodes was determined to be the trained network with the lowest ASE value of the experiment datasets [56]. Following optimisation, the best network was trained using both the training and testing datasets to provide the interconnecting link weights for the train-all model. By contrasting with the model's outputs, datasets that had not been used to train the network were used to test and validate the model. A 2-n-1 ANN model schematic (two inputs, one output, n hidden nodes) is shown in Fig. 5. Equations 2 and 3 can also be used to express the mathematical equations of the 2-n-1 ANN models. Also, the flowchart shown in Fig. 6 illustrates the ANN modelling procedure.

Table 5 Characteristics of the datasets

Parameter (unit)	Max	Min	Mean	Standard deviation
T (°C)	800	23	–	–
UPV (m/sec)	4873	203	2460.6	1452.05
SS (MPa)	5.67	1.16	3.23	1.33

Table 6 Inputs and outputs of the ANN model

	Parameter	Definition
Inputs	Tn	Normalized temperature
	UPVn	Normalized ultrasonic pulse velocity
Output	SSn	Normalized concrete splitting strength

Fig. 5 Schematic of 2 inputs, n hidden nodes, and 1 output ANN model
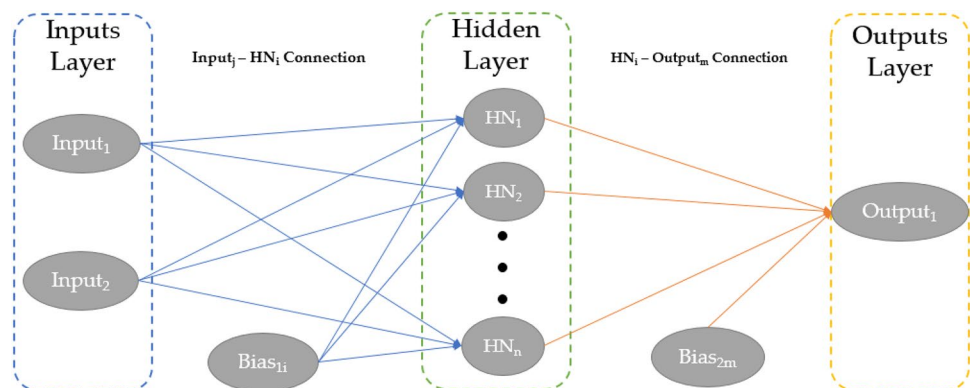
Fig. 6 ANN modelling procedure flowchart
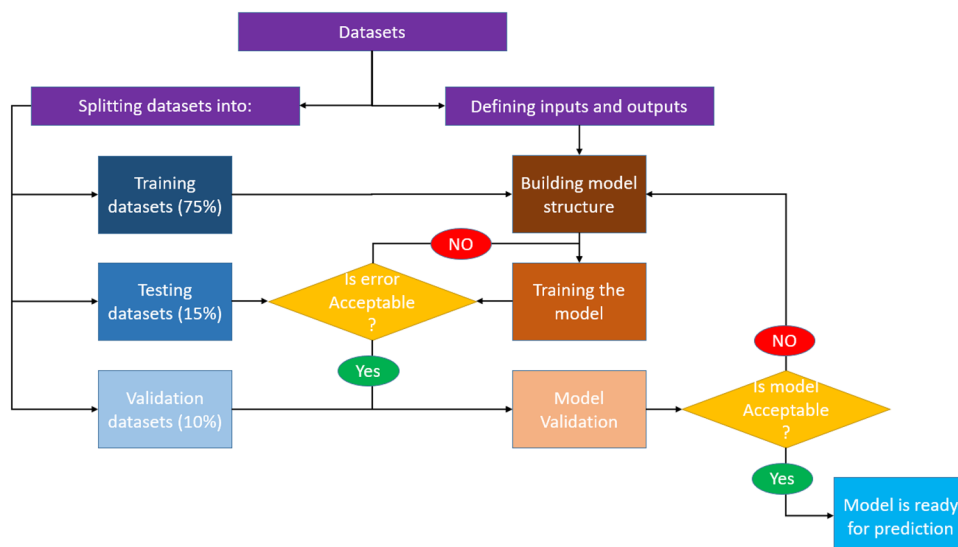
Fig. 7 Accuracy measurements of training and testing data for the developed ANN model (**a**) number of hidden nodes VS average squared error (**b**) number of hidden nodes VS mean average relative error (**c**) number of hidden nodes VS R^2

a) ASE

b) MARE

c) R^2
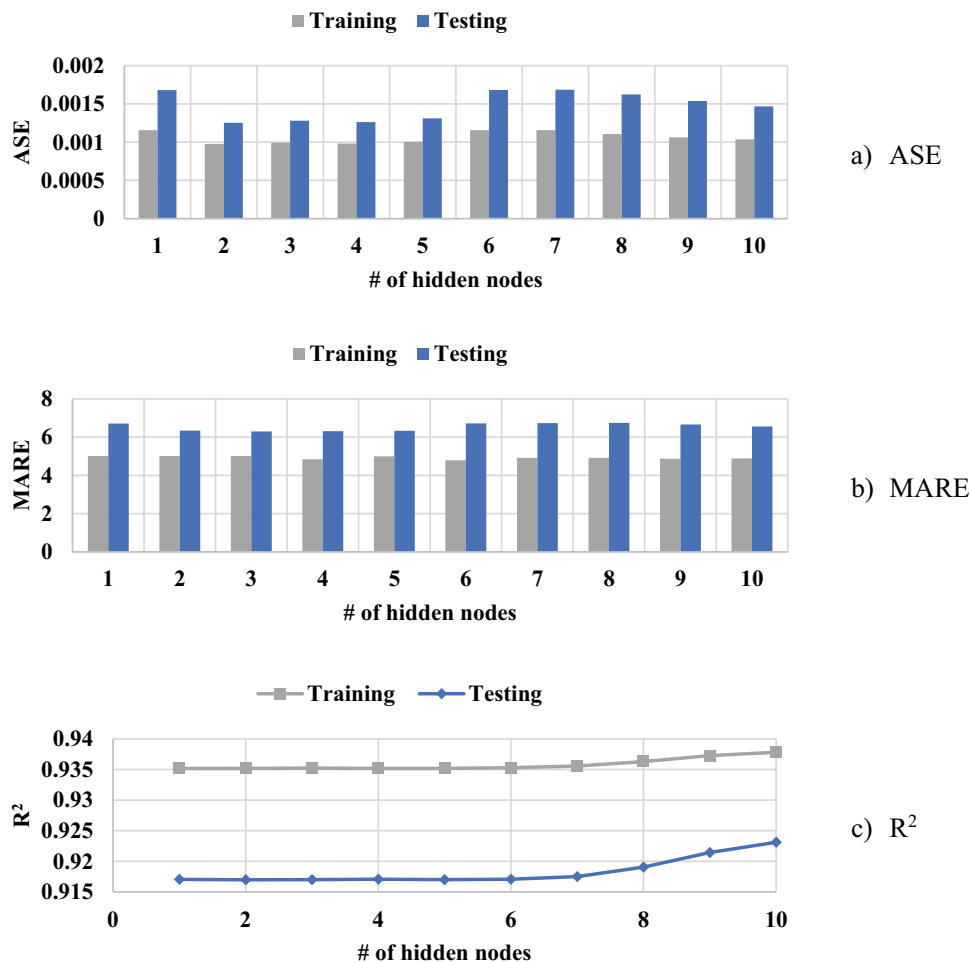
4.2 Optimizing and training the model

A total of 108 datasets were used for network optimisation. Furthermore, 18 datasets were used for testing, and 90 datasets were used to train the model. Figure 7 displays the accuracy of the ANN model training and testing using various hidden node counts. As seen, the optimal number of hidden nodes for the network was observed to be two as it had the lowest $ASE_{testing}$ value. Therefore, the architecture of the model was 2-2-1 with $ASE_{training} = 0.000978$, $ASE_{testing} = 0.001252$, $MARE_{training} = 5.0097$, $MARE_{testing} = 6.3412$, $R^2_{training} = 0.93519$, and $R^2_{testing} = 0.91698$.

All training and testing datasets were employed in model training to optimise the interconnecting link weights after the model structure had been defined. The final model was trained on a total of 108 training and testing datasets and its accuracy was as follows: $ASE = 0.000907$, $MARE = 5.028$, and $R^2 = 0.9431$. Table 6 shows the interconnecting link weights among the network nodes. Also, for validation, a k-fold (k = 12 folds) cross validation is conducted and the mean square error is calculated. The SS values are distributed randomly in 12 folds, 11 used for training and the last for validation. This process was repeated 12 times where each fold was used for validation for once and the mean square error is calculated for the validation fold. Figure 8 lists the mean square error values for each validation fold and the average for all folds. Based on the k-fold cross validation, fold 2 is used for model training and fold 12 for validation. Table 7 lists the connection links weights between the inputs, hidden nodes, and output in the optimized 2–2–1 ANN model.

4.3 Model validation

Twelve validation datasets that had not been used during training were used to validate the model. The accuracy of the validation datasets was computed and found to be $ASE_{validation} = 0.000639$, $MARE_{validation} = 4.995$, and $R^2_{validation} = 0.9169$. Additionally, Fig. 9 displays the experimental datasets in comparison to the training, testing, and validation datasets' ANN predictions. The validation predicted vs experimental data results and validation accuracy measurements show that 2-2-1 ANN model predictions were significantly plausible and satisfactory.

4.4 Simulation

Based on the ANN modeling and to illustrate the correlation between UPV, temperature, and SS, a mapping chart was created using the formulated ANN model. The correlation between the UPV, temperature, and SS of damaged concrete is depicted in Fig. 10. The relations between T, UPV and SS conducted from the ANN modelling came in a good agreement with the experimental results.

5 Conclusions

In this comprehensive study, an extensive experimental testing program that encompassed several critical aspects of concrete behavior under high-temperature conditions was conducted. This program involved the casting of diverse concrete mixtures, subjecting them to a wide temperature range spanning from 200 to 800 °C, and performing measurements of Ultrasonic Pulse Velocity (UPV) along with tensile splitting strength (SS) tests. Additionally, an Artificial Neural Network (ANN) model was developed and rigorously validated to establish a robust link between exposure temperature, UPV, and splitting strength. The results and insights gained from this study are of significant importance:

Fig. 8. 12-Fold cross validation
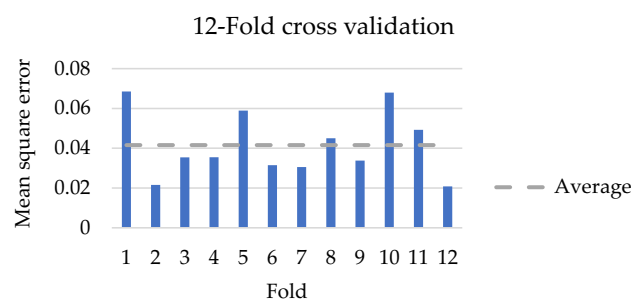
Table 7 Weight of the interconnecting links of the 2-2-1 ANN model

Input	Connection links weights between inputs and hidden nodes ($Input_j$—HN_i connection)	
	HN_1	HN_2
Tn	1.673	− 0.39354
UPVn	4.3654	− 0.31556
$Bias_{1i}$	− 2.7331	− 0.260594
$Output_m$	Connection links weights between hidden nodes and outputs (HN_i – $Output_m$ connection)	
	HN_1	HN_2	$Bias_{2m}$
SSn	5.6925	− 0.036248	− 3.48625

Fig. 9 Training and validation prediction results of the 2-2-1 ANN model vs experimental results
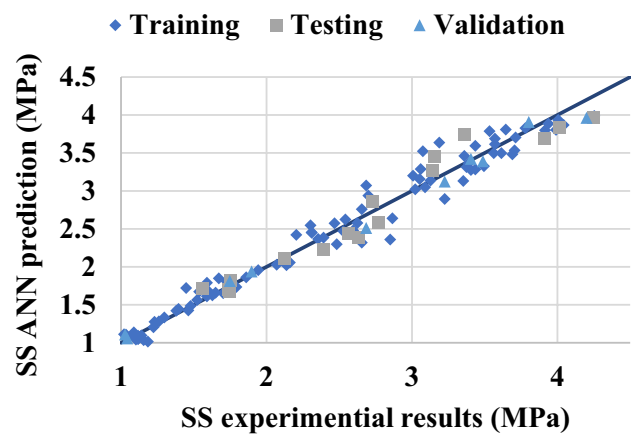
Fig. 10 Contour mapping between UPV, T, and SS
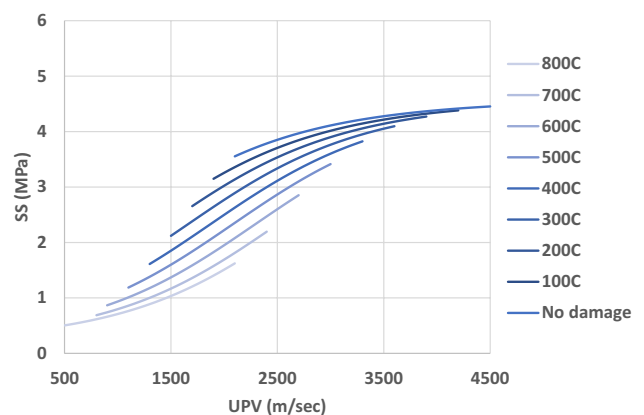
- Temperature impact on splitting strength: It was unequivocally demonstrated that exposing concrete to varying temperatures had a profound effect on its splitting strength. Notably, at the extreme temperature of 800 °C, the concrete's splitting strength exhibited a staggering reduction of 75%. This finding underscores the critical importance of considering temperature conditions when designing and assessing concrete structures, especially in environments prone to high-temperature exposures.

- High-temperature effects on UPV: this research illuminated the clear influence of elevated temperatures, particularly at 200 °C and above, on Ultrasonic Pulse Velocity (UPV). This effect provides valuable insight into the non-destructive assessment of concrete integrity under high-temperature conditions, aiding in the early detection of potential issues.

- ANN model performance: The developed ANN model, characterized by an impressive R^2 value of 0.97, effectively captured and simulated the intricate relationship between UPV, temperature, and the splitting strength of concrete subjected to high-temperature damage. This achievement highlights the potential of artificial intelligence and machine learning approaches in predicting concrete behavior in complex scenarios.

- Practical implications: The findings from this study have direct practical applications for professionals in the field of construction and structural engineering. These insights can be instrumental in adapting concrete mix designs based on anticipated temperature exposures, enhancing the oversight of structures operating in high-temperature environments, and evaluating the condition of concrete components damaged by fire. By leveraging this knowledge, practitioners can make informed decisions that not only optimize performance but also ensure the safety and longevity of concrete structures.

In summary, this study's multifaceted approach, combining experimental testing with advanced modeling techniques, has expanded our understanding of concrete behavior under extreme temperature conditions. These findings are poised to empower professionals in the construction industry to make informed choices and design resilient structures capable of withstanding the challenges posed by high-temperature exposures.

Data availability Manuscript data are included in its body.

Declarations

Competing interests The author declares that he has no conflict of interest in relation to this research, whether financial, personal, authorship or otherwise, that could affect the research and its results presented in this paper.

References

1. Hager I. Behaviour of cement concrete at high temperature. Bull Polish Acad Sci: Tech Sci. 2013;61(1):145–54.
2. Jiang Z, He B, Zhu X, Ren Q, Zhang Y. State-of-the-art review on properties evolution and deterioration mechanism of concrete at cryogenic temperature. Constr Build Mater. 2020;257:119456.
3. Sudarshan DK, Vyas AK. Impact of fire on mechanical properties of concrete containing marble waste. J King Saud Univ Eng Sci. 2019;31(1):42–51.
4. Haddad RH, Almasaeid HH. Recovering shear capacity of heat-damaged beams using NSM-CFRP strips. Constr Build Mater. 2016;105:448–58.
5. Khoury GA. Compressive strength of concrete at high temperatures: a reassessment. Mag Concr Res. 1992;44(161):291–309.
6. Almasaeid HH, Suleiman A, Alawneh R. Assessment of high-temperature damaged concrete using non-destructive tests and artificial neural network modelling. Case Stud Constr Mater. 2022;16: e01080.
7. Malik M, Bhattacharyya SK, Barai SV. Thermal and mechanical properties of concrete and its constituents at elevated temperatures: a review. Constr Build Mater. 2021;270: 121398.
8. Mathews ME, Kiran T, Naidu VCH, Jeyakumar G, Anand N. Effect of high-temperature on the mechanical and durability behaviour of concrete. Mater Today Proc. 2021;42:718–25.
9. Khaliq W, Kodur VKR. Effect of high temperature on tensile strength of different types of high-strength concrete. ACI Mater J. 2011;108(4):394–403.
10. Wang Y, Liu F, Xu L, Zhao H. Effect of elevated temperatures and cooling methods on strength of concrete made with coarse and fine recycled concrete aggregates. Constr Build Mater. 2019;210:540–7.
11. Krishna DA, Priyadarsini RS, Narayanan S. Effect of elevated temperatures on the mechanical properties of concrete. Proc Struct Integr. 2019;14:384–94.
12. Ali F, Nadjai A, Silcock G, Abu-Tair A. Outcomes of a major research on fire resistance of concrete columns. Fire Saf J. 2004;39(6):433–45.
13. Bilodeau A, Kodur VKR, Hoff GC. Optimization of the type and amount of polypropylene fibres for preventing the spalling of lightweight concrete subjected to hydrocarbon fire. Cement Concr Compos. 2004;26(2):163–74.
14. Karatas M, Dener M, Benli A, Mohabbi M. High temperature effect on the mechanical behavior of steel fiber reinforced self-compacting concrete containing ground pumice powder. Struct Concr. 2019;20(5):1734–49.
15. Ahmed M, Mallick J, Hasan MA. A study of factors affecting the flexural tensile strength of concrete. J King Saud Uni Eng Sci. 2016;28(2):147–56.
16. Kodur VJSP. Fiber reinforced concrete for enhancing structural fire resistance of columns. Spec Publ. 1999;182:215–34.
17. Behnood A, Ghandehari M. Comparison of compressive and splitting tensile strength of high-strength concrete with and without polypropylene fibers heated to high temperatures. Fire Saf J. 2009;44(8):1015–22.
18. Shariati M, Ramli-Sulong NH, Arabnejad MM, Shafigh P, Sinaei H. Assessing the strength of reinforced concrete structures through Ultrasonic Pulse Velocity and Schmidt Rebound Hammer tests. Sci Res Essays. 2011;6(1):213–20.
19. Malek J, Kaouther M. Destructive and non-destructive testing of concrete structures. Jordan J Civ Eng. 2014;8(4):432–41.
20. Almasaeid H, Alkasassbeh A, Yasin B. Prediction of geopolymer concrete compressive strength utilizing artificial neural network and nondestructive testing. Civ Environ Eng. 2022;18:655–65.
21. Martins Filho ST, Bosquesi EM, Fabro JR, Pieralisi R. Characterization of pervious concrete focusing on non-destructive testing. Revista IBRACON de Estruturas e Materiais. 2020;13:483–500.
22. Rajabi AM, Omidi Moaf F, Abdelgader HS. Evaluation of mechanical properties of two-stage concrete and conventional concrete using nondestructive tests. J Mater Civ Eng. 2020;32(7):04020185.
23. Tripathi D, Kumar R, Mehta PK, Singh A. Evaluation of a sustainable self compacting concrete using destructive and non-destructive testing. Mater Today Proc. 2022;58:830–5.

24. Trtnik G, Kavčič F, Turk G. Prediction of concrete strength using ultrasonic pulse velocity and artificial neural networks. Ultrasonics. 2009;49(1):53–60.
25. Huismann S, Weise F, Schneider U. Influence of the preload on the mechanical properties of high strength concrete at high temperatures. In 1st International workshop on concrete spalling due to fire exposure. 2009. pp. 189–200.
26. Colombo M, Felicetti R. New NDT techniques for the assessment of fire-damaged concrete structures. Fire Saf J. 2007;42(6–7):461–72.
27. Abed M, de Brito J. Evaluation of high-performance self-compacting concrete using alternative materials and exposed to elevated temperatures by non-destructive testing. J Build Eng. 2020;32: 101720.
28. Chung HW. Ultrasonic testing of concrete after exposure to high temperatures. NDT Int. 1985;18(5):275–8.
29. Lehner P, Hrabová K. Relationship of time-dependent parameters from destructive and non-destructive tests of structural concrete. Mathematics. 2022;10(3):460.
30. Abdallah W, Sbartaï ZM, Saliba J, Elachachi SM, Chehade FH, Sadek M. Assessment of the reliability of concrete evaluation by multi-physical inversion of NDT measurements—a probabilistic approach. Constr Build Mater. 2021;300: 124371.
31. Fausett LV. Fundamentals of neural networks: architectures, algorithms and applications. Pearson Education India. 2006.
32. Khan S, Rahmani H, Shah SAA, Bennamoun M, Medioni G, Dickinson S. A guide to convolutional neural networks for computer vision, vol. 8. San Rafael: Morgan & Claypool Publishers; 2018. p. 1–207.
33. Sami BHZ, Sami BFZ, Kumar P, Ahmed AN, Amieghemen GE, Sherif MM, El-Shafie A. Feasibility analysis for predicting the compressive and tensile strength of concrete using machine learning algorithms. Case Stud Constr Mater. 2023;18: e01893.
34. Nguyen H, Vu T, Vo TP, Thai HT. Efficient machine learning models for prediction of concrete strengths. Constr Build Mater. 2021;266: 120950.
35. Kouddane B, Sbartaï ZM, Alwash M, Ali-Benyahia K, Elachachi SM, Lamdouar N, Kenai S. Assessment of concrete strength using the combination of NDT—review and performance analysis. Appl Sci. 2022;12(23):12190.
36. Silva FA, Delgado JM, Cavalcanti RS, Azevedo AC, Guimarães AS, Lima AG. Use of nondestructive testing of ultrasound and artificial neural networks to estimate compressive strength of concrete. Buildings. 2021;11(2):44.
37. Demir A. Prediction of hybrid fibre-added concrete strength using artificial neural networks. Comput Concr. 2015;15(4):503–14.
38. Atici U. Prediction of the strength of mineral admixture concrete using multivariable regression analysis and an artificial neural network. Expert Syst Appl. 2011;38(8):9609–18.
39. Bui DK, Nguyen T, Chou JS, Nguyen-Xuan H, Ngo TD. A modified firefly algorithm-artificial neural network expert system for predicting compressive and tensile strength of high-performance concrete. Constr Build Mater. 2018;180:320–33.
40. Ray S, Haque M, Ahmed T, Nahin TT. Comparison of artificial neural network (ANN) and response surface methodology (RSM) in predicting the compressive and splitting tensile strength of concrete prepared with glass waste and tin (Sn) can fiber. J King Saud Univ Eng Sci. 2021;35(3):185–99.
41. Behnood A, Verian KP, Gharehveran MM. Evaluation of the splitting tensile strength in plain and steel fiber-reinforced concrete based on the compressive strength. Constr Build Mater. 2015;98:519–29.
42. Candelaria MDE, Kee SH, Lee KS. Prediction of compressive strength of partially saturated concrete using machine learning methods. Materials. 2022;15(5):1662.
43. Rajczakowska M, Szeląg M, Habermehl-Cwirzen K, Hedlund H, Cwirzen A. Interpretable machine learning for prediction of post-fire self-healing of concrete. Materials. 2023;16(3):1273.
44. Kasperkiewicz J. Prediction of concrete properties using neural networks. Eng Trans. 1997;45(2):251–63.
45. Candelaria MDE, Chua NMM, Kee SH. Evaluation of heat-induced damage in concrete using machine learning of ultrasonic pulse waves. Materials. 2022;15(22):7914.
46. Komlos K, Popovics S, Nürnbergerová T, Babal B, Popovics JS. Ultrasonic pulse velocity test of concrete properties as specified in various standards. Cement Concr Compos. 1996;18(5):357–64.
47. Breccolotti M, Bonfigli MF. I-SonReb: an improved NDT method to evaluate the in situ strength of carbonated concrete. Nondestruct Test Eval. 2015;30(4):327–46.
48. Sutan NM, Meganathan M. A comparison between direct and indirect method of ultrasonic pulse velocity in detecting concrete defects. J Nondestr Test. 2003;8(5):1–9.
49. Ahmed AM. Prediction of dissolved oxygen in Surma River by biochemical oxygen demand and chemical oxygen demand using the artificial neural networks (ANNs). J King Saud Univ Eng Sci. 2017;29(2):151–8.
50. Abiodun OI, Jantan A, Omolara AE, Dada KV, Umar AM, Linus OU, et al. Comprehensive review of artificial neural network applications to pattern recognition. IEEE Access. 2019;7:158820–46.
51. Najjar YM, Basheer IA, Mcreynolds R. Neural modeling of Kansas soil swelling. Transp Res Rec. 1996;1526(1):14–9.
52. Krose B, Smagt P. An introduction to neural networks. Amesterdam, Netherland: University of Ámsterdam; 1996. p. 29.
53. Ahmadi M, Naderpour H, Kheyroddin A. Utilization of artificial neural networks to prediction of the capacity of CCFT short columns subject to short term axial load. Arch Civ Mech Eng. 2014;14(3):510–7.
54. Sharifzadeh M, Sikinioti-Lock A, Shah N. Machine-learning methods for integrated renewable power generation: a comparative study of artificial neural networks, support vector regression, and Gaussian Process Regression. Renew Sustain Energy Rev. 2019;108:513–38.
55. Allouzi RA, Almasaeid HH, Salman DG, Abendeh RM, Rabayah HS. Prediction of bond-slip behavior of circular/squared concrete-filled steel tubes. Buildings. 2022;12(4):456.
56. Almasaeid HH, Salman DG. Application of artificial neural network to predict the properties of permeable concrete. Civ Eng Archit. 2022;10(6):2292–305.